Theory of Light-Ion Acceleration Driven by a Strong Charge Separation

M. Passoni[1,2] and M. Lontano[2]

[1]Dipartimento di Chimica Materiali e Ingegneria Chimica "G. Natta," Politecnico di Milano, and Sezione di Milano INFN, Milan, Italy

[2]Istituto di Fisica del Plasma, Consiglio Nazionale delle Ricerche, Milan, Italy

(Received 11 April 2008; published 10 September 2008)

A theoretical model of the quasistatic electric field, formed at the rear surface of a thin solid target irradiated by a ultraintense subpicosecond laser pulse, due to the appearance of a cloud of ultrarelativistic bound electrons, is developed. It allows one to correctly describe the spatial profile of the accelerating field and to predict the maximum energies and the energy spectra of the accelerated ions. The agreement of the theoretical expectations with the experimental data looks satisfactory in a wide range of conditions. Previsions of regimes achievable in the future are given.

DOI: 10.1103/PhysRevLett.101.115001 PACS numbers: 52.38.Kd, 52.27.Ny, 52.40.Kh

Laser-induced ion acceleration seems to be one of the most promising applications of the interaction of ultraintense ultrashort laser pulses with solid matter [1]. Several processes can be responsible for laser ion acceleration, depending on the laser intensity [2]. Most of the present experiments rely on the so-called target normal sheath acceleration (TNSA) mechanism [3]. The optimization of the interaction conditions requires the formulation of a first-principle physical model of the acceleration, to properly choose the laser-target parameters and optimize and control the ion properties. To this aim, we have developed a consistent theoretical description of the spatial distribution of the electron cloud at the rear surface of a planar target irradiated by a powerful laser on the front side. We look for a quasistationary solution of the Poisson equation, where the source charge is represented by the laser produced, hot electron population. The model is assumed to be valid on times shorter than the typical time scales (a few times $2\pi\omega_{\rm pi}^{-1}$) over which the ions present in the solid target respond collectively to the space charge. The interest for this transient equilibrium solution is that the most energetic ions are accelerated, basically as test particles, by this fully developed relativistic electron cloud, before it is partially short-circuited by the positive ion current and before the electron temperature starts decreasing due to electron-ion collisions and radiative losses. In this respect, our analysis is complementary to the model developed by Mora [4,5], which is used to describe the fluid non-neutral "target expansion" of a one-component plasma over tens of $\omega_{\rm pi}^{-1}$, a relatively long time over which the bulk of light ions follow the expansion of the electron cloud, either behaving isothermally [4] or adiabatically cooling down [5]. On the contrary, immediately after the laser interaction ($t \leq \omega_{\rm pi}^{-1}$), a huge charge separation is produced, which imparts the maximum impulse to the lightest ions (e.g., a thin surface layer of contaminant protons), the first and most efficiently accelerated in a system where the heaviest target ions remain almost immobile over this time scale [6–8]. Several other theoretical studies of the TNSA mechanism have been recently carried out [9–14]. All of these models foresee that the accelerating electric field extends up to $\xi \to \infty$, although results of particle-in-cell simulations and the experimental evidence [15] indicate that it goes to zero at a finite short distance (of about 20 μm in the considered cases) from the rear surface, at least during the acceleration of the most energetic ions. A related problem is that in Refs. [4,5,14], the self-consistent electrostatic potential diverges to $-\infty$ at large distance from the target, which introduces the need of defining artificially a finite acceleration time and/or limited region over which the acceleration is effective. As a consequence, the fitted acceleration times, assumed equal or directly related to the laser pulse duration τ_L [13,16], usually do not correspond to the physical times over which ion acceleration takes place when $\tau_L < 100$ fs, which has become a quite usual experimental condition. For these regimes, *ad hoc* fittings are required [17]. The basic idea of this Letter is that only those electrons, which are bound in the overall positive potential created by the lattice ions and by themselves, participate to the formation of the quasistationary electron cloud, while the most energetic electrons overcome the potential barrier and are lost by the system [7,18,19]. As we shall see, the correct inclusion of the *bound electrons* only in the Poisson equation removes all the above mentioned problems, leading all physical quantities to become zero at a finite distance from the rear surface. Our model, whose principle has been discussed in Refs. [7,20] for the nonrelativistic case, $p \ll mc$, is now extended to the ultrarelativistic case in order to be applied to present experimental situations. Its predictions have been compared with the maximum ion energies and spectra observed in recent experiments, characterized by different regimes, with overall satisfactory agreement. It has also been used to predict the achievable ion parameters with future powerful lasers.

Assume a uniform ion distribution in the interval $-d \leq x \leq 0$, representing the target lattice of finite extent d.

 © 2008 The American Physical Society

Ideally, an ultraintense laser is shot onto the front surface, at $x = -d$, where it produces a hot electron population which expands freely through the foil and appears at the rear surface, $x = 0$, where it achieves a quasisteady equilibrium for a time of the order of hundreds of femtoseconds, before the first proton- (or more generally ion-) layer starts being accelerated into the half space $x > 0$ and before electron cooling takes place. We expect that hot electrons with negative total energy W, that is with $-e\phi(x) < W < 0$, remain close to the rear surface $x = 0$ (that is are "bound" or "trapped") thus forming a negatively charged hot electron cloud extending outside of the target. On the contrary, the most energetic electrons ("free" electrons with $W > 0$), are lost by the system [18,19,21] and do not contribute to the ion acceleration. Our aim is to describe this quasistationary state at the rear surface, looking for a stationary solution of the Poisson equation. Note that the properties induced by the trapped electrons have recently received great attention for their role in the spatial control of the ion beam [21]. Consider the one-dimensional Maxwell-Jüttner relativistic electron distribution function (EDF) in the self-consistent electrostatic potential $\phi(x)$, $F_e(x, p) = \tilde{n}/[2mcK_1(\zeta)] \times \exp[-(W + mc^2)/T]$, where $W = mc^2(\gamma - 1) - e\phi$, T is the hot electron temperature, $K_1(\zeta)$ is the MacDonald function of 1st order and argument $\zeta = mc^2/T$, m the rest electron mass, e the modulus of the electron charge, c the speed of light, $\gamma = (1 + p^2/m^2c^2)^{1/2}$, and the EDF has been normalized to the density $\tilde{n}$ by integrating over $-\infty < p < +\infty$. In $x \geq 0$ the source in the Poisson equation is given by the bound electron charge density

$$n_b(x) = \int_{W<0} F_e(x, p)dp, \tag{1}$$

where the integration extends over the negative energies only. To proceed analytically, we assume that at sufficiently large laser intensities the EDF can be well approximated by its ultrarelativistic limit. Therefore, we consider the inequality $p/mc \gg 1$, leading to a simplified expression of the EDF,

$$F_e(x, p) \approx \frac{\tilde{n}}{2mcK_1(\zeta)} \exp\left[-\frac{c|p| - e\phi}{T}\right]. \tag{2}$$

The "bound" electron density is consistently calculated by integrating Eq. (2) over $0 < |p| < e\phi/c$, which gives

$$n_b(x) = \frac{\tilde{n}T}{mc^2K_1}\left[\exp\left(\frac{e\phi}{T}\right) - 1\right]. \tag{3}$$

Let us introduce the following dimensionless variables: $\xi = x/\lambda_D$, $\varphi = e\phi/T$, where $\lambda_D^2 = mc^2K_1/(4\pi\tilde{n}e^2)$. The Poisson equation for $\xi \geq 0$ can be integrated once giving

$$\frac{d\varphi}{d\xi} = -\sqrt{2}(e^{\varphi} - \varphi - 1)^{1/2}; \tag{4}$$

here the constant has been determined by imposing that a $\tilde{\xi}$ exists where $\varphi(\tilde{\xi}) = \varphi' = \varphi'' = 0$. A further integration gives the implicit relation between φ and ξ:

$$\int_{\varphi_0}^{\varphi(\xi)} \frac{d\varphi}{(e^{\varphi} - \varphi - 1)^{1/2}} = -\sqrt{2}\xi, \tag{5}$$

where $\varphi_0 = \varphi(\xi = 0)$. For $|\varphi(\xi)| \ll 1$, that is far from the rear surface, Eq. (5) gives $\varphi(\xi) \approx \varphi_0 e^{-\xi}$, which should go continuously into that discussed in Ref. [7] for the nonrelativistic case, had the exact form of the EDF been used. The analysis in Ref. [7] predicts a finite spatial extent of the electron cloud ($\tilde{\xi} \approx \sqrt{6\sqrt{\pi}\varphi_0^{1/4}}$), in quantitative agreement with experimental observations [15]. In the opposite limit $|\varphi(\xi)| \gg 1$, occurring close to $\xi = 0$, $\varphi(\xi) \approx \varphi_0 - 2\ln[1 + \xi/\sqrt{2}\exp(\varphi_0/2)]$. From Eq. (4), the normalized electric field at $\xi = 0$ can be calculated as $E = [2\exp(\frac{\varphi_0}{2})]/[\sqrt{2} + \xi\exp(\frac{\varphi_0}{2})]$. The implicit solution of Eq. (5) depends on the φ_0, that can be determined by solving the Poisson equation in the target, for $\xi < 0$, and imposing the continuity of φ and of φ' at $\xi = 0$.

For $x < 0$ the net charge density is $n_e - Zn_i$. Generally speaking, besides the hot electron population n_b and the full ion species, a cold electron species n_c is also present which will be considered at zero temperature. The electric field source is $n_b - (Zn_i - n_c)$, where the content of the parenthesis is assumed as a given constant. The Poisson equation then writes

$$\frac{d^2\varphi^<}{d\xi^2} = e^{\varphi^<} - 1 - B, \tag{6}$$

where $\varphi^<$ represents the normalized potential for $\xi < 0$, and $B = (Zn_i - n_c)/(T\tilde{n}/mc^2K_1)$. We assume that, far from $\xi = 0$ inside the target, the plasma becomes locally quasineutral, so that $B \cong e^{\varphi*} - 1$, where $\varphi* = \varphi^<(\xi = -\xi_d = -d/\lambda_D)$. By integrating once Eq. (6) we get

$$\frac{d\varphi^<}{dx} = -\sqrt{2}[e^{\varphi^<} + e^{\varphi*}(\varphi* - 1 - \varphi^<)]^{1/2}, \tag{7}$$

where the condition of $E = 0$ at $\xi = -\xi_d$ has been imposed. Equating the expressions of the electric field at $\xi = 0$ from Eqs. (4) and (7) determines a relation between φ_0 and $\varphi*$, that is

$$\varphi_0 = \frac{e^{\varphi*}(\varphi* - 1) + 1}{e^{\varphi*} - 1}. \tag{8}$$

The electrostatic potential is fully determined from Eq. (5) once $\varphi*$ is given. If a test ion of charge Z is placed at rest at $\xi = 0$, it is accelerated up to a maximum kinetic energy $\epsilon_{i,\max} = Z\varphi_0 = E_i^{\text{mod}}/T$. Assume that a small number of ions at rest, with constant surface density N_i, are distributed uniformly in a thin layer placed in $0 \leq \xi \leq \delta\xi$, with $\delta\xi \ll \xi_d$; their volume density is $n_\xi(\xi) = (N_i/\delta\xi) \times [H(\xi) - H(\xi - \delta\xi)]$. The ion energy distribution after crossing the hot electron cloud is

TABLE I. The main laser and proton parameters introduced in the text are collected from several published data. For relatively long laser pulses, i.e., $\tau_L = 0.5$ ps [1], 0.7 ps [23], 0.9 ps [24], $\lambda = 1\ \mu$m; otherwise, $\lambda = 0.8\ \mu$m.

Ref.	E_L	τ_L	I_L	$E_{\rm pr}^{\rm mea}$	$E_{\rm pr}^{\rm mod}$	$\Delta E/E$
[1]	500	500	3×10^{20}	58	61, 7	6.5%
[23]	400	700	2×10^{20}	44	48.6	10%
[25]	10	100	1×10^{20}	24	21.9	8.9%
[26]	0.84	40	6×10^{19}	9.5	8.5	10%
[27]	0.6	150	1×10^{19}	2.5	2.4	4.8%
[27]	0.85	150	1.5×10^{19}	4	3.4	15%
[28]	0.25	70	3×10^{18}	0.88	0.78	11%
[24]	50	900	5×10^{19}	18	18.1	<1%
[29]	0.1	60	6.8×10^{18}	1.2	1.12	6.6%
[30]	0.2	60	7×10^{18}	1.5	1.39	7.3%

$$n_\epsilon(\epsilon) = \frac{n_\xi(\xi)}{d\epsilon/d\xi} = \frac{N_i}{\delta\epsilon}\frac{(e^{\epsilon_0/Z} - \frac{\epsilon_0}{Z} - 1)^{1/2}}{(e^{\epsilon/Z} - \frac{\epsilon}{Z} - 1)^{1/2}} S(\epsilon), \qquad (9)$$

where $S(\epsilon) = H(\epsilon - \epsilon_0) - H(\epsilon - \epsilon_0 - \delta\epsilon)$ is a combination of Heaviside functions, $\epsilon = Z\varphi$, $\delta\epsilon = Z\delta\varphi$, and $\delta\varphi \ll \varphi_0$ is assumed. The quantity $\varphi*$ represents the normalized maximum electron energy of the laser produced trapped electrons $\epsilon_{e,\max} = K_{e,\max}/T$. It depends on the physics of the laser-electron coupling, a problem which is out of the scope of the present analysis. Alternatively, it can be related to experimental data, or taken from suitable numerical simulations, or determined on physical ground. Here, we propose a scaling law relating $\epsilon_{e,\max}$ with E_L, based on the analysis of published results [22]:

$$\epsilon_{e,\max} = \frac{K_{e,\max}}{T} \approx A + B\ln[E_L(J)], \qquad (10)$$

where $A = 4.8$ and $B = 0.8$. Equation (8) is used to infer $K_{e,\max}$ from the observed maximum ion energy. This procedure leads to Eq. (10), which, together with Eqs. (8) and (9), allows one to make predictions for future experiments. In Table I a collection of examples from various published experiments, characterized by different laser parameters, is presented, comparing the maximum observed proton energies $E_{\rm pr}^{\rm mea}$ with the predictions of our model $E_{\rm pr}^{\rm mod}$ (in MeV). $E_L(J)$, τ_L(fs), $I_L({\rm W\,cm^{-2}})$, and $E_{\rm pr}^{\rm mea}$ for each case, together with $E_{\rm pr}^{\rm mod}$ and $\Delta E/E = |E_{\rm pr}^{\rm mod} - E_{\rm pr}^{\rm mea}|/E_{\rm pr}^{\rm mea}$ are shown. T is estimated on the basis of the ponderomotive expression [3]. The agreement is always satisfactory, the relative error staying below 10% in most cases. It is worth noting how the physical behavior emerging from so different laser parameters ($0.1 < E_L < 500$ J, $40 < \tau_L < 900$ fs, $3\times10^{18} < I_L < 3\times10^{20}\ {\rm W\,cm^{-2}}$) is satisfactorily captured within our theoretical model.

Equations (9) and (10) have been also used to calculate, for three different experimental arrangements, the proton energy spectra resulting from the acceleration of a 50 nm thin proton layer of diameter $D = 2R = f_L + d\tan\theta$ (f_L and θ are the focal spot diameter and the divergence angle of the electrons crossing the target) and density equal to $\alpha\times10^{22}\ {\rm cm^{-3}}$ (α is of the order of unity and depends on the particular experimental conditions), located at rest on the rear surface. Two high laser intensity experiments [1,23] and a relatively low intensity one [28] have been considered. In Fig. 1, the ion energy spectra taken from Refs. [1] (a), [23] (b), and [28] (c), with the spectra obtained from Eq. (9) superimposed, are presented. It can be seen how both the maximum proton energies $E_{\rm pr}$ and the upper energy cutoff in the spectra are well reproduced. To further test the generality of the theory, we considered also recent results about acceleration of a quasimonoenergetic beam of C ions [31]. We obtained satisfactory agreement both for the maximum energy (theory: 33 MeV, experiment: 36 MeV) and for the ion spectrum (not shown).

A particularly interesting situation is provided by very recent experimental results showing new features about TNSA, arising when ultrahigh contrast (UHC) pulses are used [32,33]. For UHC $>10^{10}$, it becomes possible to use ultrathin targets in the sub-μm range. In such systems a significant enhancement in the maximum ion energy has been observed, compared to what can be obtained with the

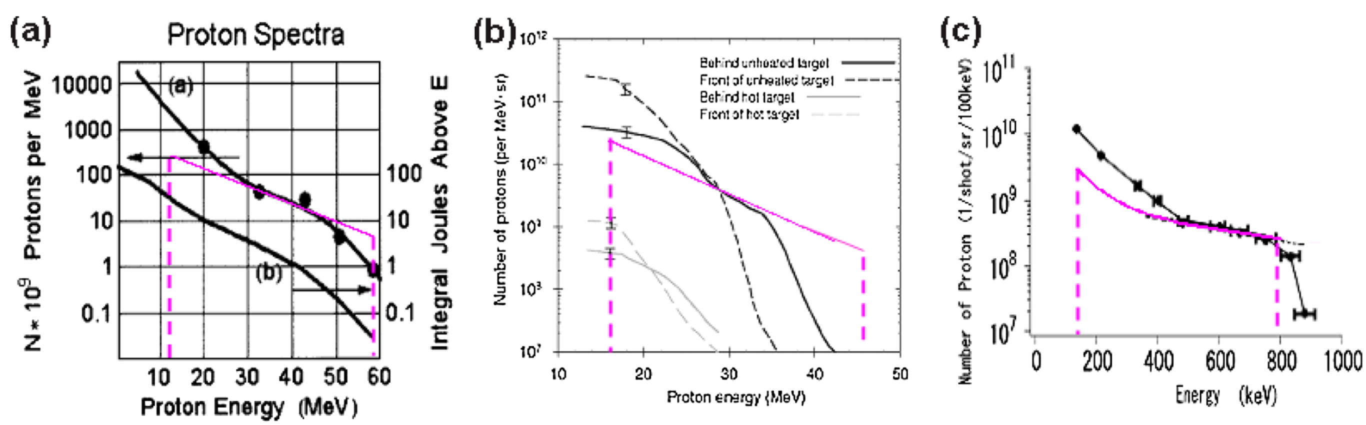

FIG. 1 (color online). Proton energy spectra n_ϵ vs ϵ (in MeV, color lines) from Eq. (9) superimposed to measured spectra taken from Refs. [1] (a), [23] (b), and [28] (c). See the original references for details about the measured spectra. The estimated values of $K_{e,\max}$ are 68.8 MeV (a), 54.3 MeV (b), 1.03 MeV (c), respectively.

same pulses without UHC. Numerical simulations show an increase of the maximum and mean hot electron energy produced in conditions of UHC. We used the numerical values contained in Fig. 4 of Ref. [32] ($K_{e,\max} \approx$ 3.2 MeV), and from Eq. (8) a value of $E_{\rm pr}^{\rm mod} \approx 2.9$ MeV is obtained, in excellent agreement with experiments and numerical simulations (see Fig. 5 in Ref. [32]). Moreover, taking from Fig. 4 of Ref. [32] the numerical results about the hot electron population without UHC ($K_{e,\max} \approx$ 1.8 MeV), we obtain a maximum proton energy of 1.5 MeV, still in satisfactory agreement with various evidences with similar parameters (see, e.g., Refs. [28–30] and Table I). The agreements obtained are particularly convincing since in these cases no fitting parameter has been exploited. We wish to stress that measurements of fast trapped electron properties (T and $K_{e,\max}$) would be precious to help further testing. The model has been also applied to predict the laser parameters necessary to achieve a proton acceleration up to 250–300 MeV, of interest for hadron therapy [34]. In Fig. 2, the curves at constant maximum proton energy, $E_{\rm pr}$, in the plane ($I_L\lambda^2$; E_L) are shown from 100 MeV up to 300 MeV. $E_{\rm pr} = 250$ MeV can be produced for different combinations of parameters. A possibility is (7×10^{21} W μm^2/cm^2, 50 J); assuming $\lambda =$ 0.8 μm (Ti:Sa system) and E_L uniformly contained in a spot with $f_L = 7$ μm, this corresponds to a pulse with $\tau_L = 5$ fs, $I_L = 1 \times 10^{22}$ W/cm^2, and therefore a 10 PW system. If 10^{10} particles per pulse can be used, a repetition rate of about 5 Hz is needed to meet the requirement of 10 nA current. It is interesting to note that these parameters are not so far from already commercially available systems [35]. These requirements could be possibly relaxed using UHC pulses, as previously described.

In conclusion, we have developed a theoretical model of the early stages of the TNSA process, suitable for the description of the high energy part of the spectrum of the laser-accelerated ions. We have shown, by direct comparison with available experimental and numerical data, ranging over wide intervals of laser and plasma parameters, that this theory is able to correctly predict important physical properties of the acceleration process, such as the spatial profile of the quasistatic accelerating field and the relation between the characteristics of the hot electrons and those of the accelerated ions. The reliability of the model is further demonstrated by its capability of properly interpreting new features of TNSA, such as those arising from the use of UHC laser pulses.

The authors would like to thank Dr. P. McKenna and Dr. M. Nishiuchi for their permission to use their figures. Credit is given to LLNS, Lawrence Livermore National Laboratory, and the Department of Energy under whose auspices the work described in Ref. [1] was performed.

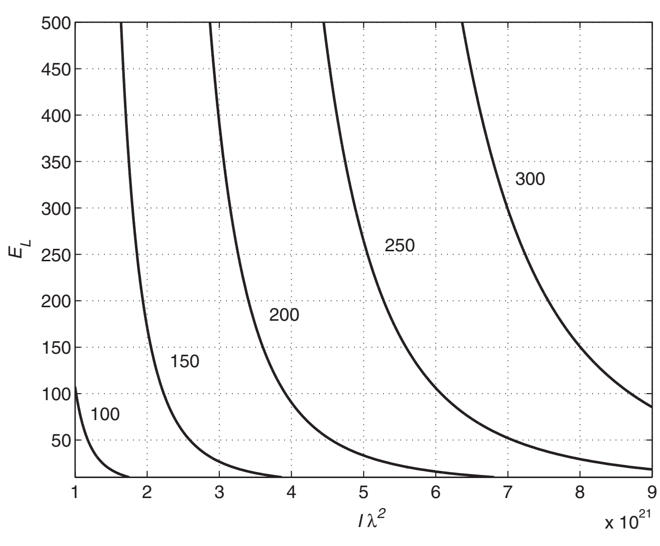

FIG. 2. The curves at constant $E_{\rm pr}^{\rm mod}$ (in MeV) are plotted in the ($I_L\lambda^2$; E_L) plane, in units (W μm^2 cm^{-2}; J).

[1] R. A. Snavely *et al.*, Phys. Rev. Lett. **85**, 2945 (2000).
[2] G. Mourou *et al.*, Rev. Mod. Phys. **78**, 309 (2006).
[3] S. C. Wilks *et al.*, Phys. Plasmas **8**, 542 (2001).
[4] P. Mora, Phys. Rev. Lett. **90**, 185002 (2003).
[5] P. Mora, Phys. Rev. E **72**, 056401 (2005).
[6] M. Passoni *et al.*, Laser Part. Beams **22**, 171 (2004).
[7] M. Lontano *et al.*, Phys. Plasmas **13**, 042102 (2006).
[8] A. P. L. Robinson *et al.*, Phys. Rev. Lett. **96**, 035005 (2006).
[9] S. Betti *et al.*, Plasma Phys. Controlled Fusion **47**, 521 (2005).
[10] P. Mora, Phys. Plasmas **12**, 112102 (2005).
[11] V. F. Kovalev *et al.*, JETP Lett. **74**, 10 (2001).
[12] M. Passoni *et al.*, Phys. Rev. E **69**, 026411 (2004).
[13] J. Schreiber *et al.*, Phys. Rev. Lett. **97**, 045005 (2006).
[14] B. J. Albright *et al.*, Phys. Rev. Lett. **97**, 115002 (2006).
[15] L. Romagnani *et al.*, Phys. Rev. Lett. **95**, 195001 (2005); also, S. V. Bulanov (private communication).
[16] J. Fuchs *et al.*, Nature Phys. **2**, 48 (2006).
[17] P. Antici, Ph.D. thesis, Ecole Polytech., France, 2007.
[18] T. E. Cowan *et al.*, Nucl. Instrum. Methods Phys. Res., Sect. A **455**, 130 (2000).
[19] M. Allen *et al.*, Phys. Plasmas **10**, 3283 (2003).
[20] Y. Kishimoto *et al.*, Phys. Fluids **26**, 2308 (1983).
[21] S. Kar *et al.*, Phys. Rev. Lett. **100**, 105004 (2008).
[22] M. Borghesi *et al.*, Fusion Sci. Technol. **49**, 412 (2006).
[23] P. McKenna *et al.*, Phys. Rev. E **70**, 036405 (2004).
[24] E. L. Clark *et al.*, Phys. Rev. Lett. **84**, 670 (2000).
[25] A. J. Mackinnon *et al.*, Phys. Rev. Lett. **88**, 215006 (2002).
[26] S. Fritzler *et al.*, Appl. Phys. Lett. **83**, 3039 (2003).
[27] M. Kaluza *et al.*, Phys. Rev. Lett. **93**, 045003 (2004).
[28] M. Nishiuchi *et al.*, Phys. Lett. A **357**, 339 (2006).
[29] T. Fujii *et al.*, Appl. Phys. Lett. **83**, 1524 (2003).
[30] I. Spencer *et al.*, Phys. Rev. E **67**, 046402 (2003).
[31] B. M. Hegelich *et al.*, Nature (London) **439**, 441 (2006).
[32] T. Ceccotti *et al.*, Phys. Rev. Lett. **99**, 185002 (2007).
[33] P. Antici *et al.*, Phys. Plasmas **14**, 030701 (2007).
[34] K. Ledingham, Nature Phys. **2**, 11 (2006).
[35] http://www.amplitude-technologies.com.